REGULAR ARTICLE

blood advances

Serglycin controls megakaryocyte retention of platelet factor 4 and influences megakaryocyte fate in bone marrow

Joshua Lykins,[1] Isabelle C. Becker,[2,3] Virginia Camacho,[2,3] Hammodah R. Alfar,[1] JoonWoo Park,[1] Joseph Italiano,[2,3] and Sidney W. Whiteheart[1]

[1]Department of Molecular and Cellular Biochemistry, University of Kentucky, Lexington, KY; [2]Department of Surgery, Boston Children's Hospital, Boston, MA; and [3]Department of Surgery, Harvard Medical School, Boston, MA

Key Points

- SRGN is necessary for PF4 retention in developing MKs.
- Marrow from Serglycin$^{-/-}$ mice have smaller MKs and decreased numbers of hematopoietic stem cells.

Megakaryocytes (MKs) produce platelets, and similar to other hematopoietic progenitors, they are involved in homeostatic aspects of their bone marrow niche. MKs release and endocytose various factors, such as platelet factor 4 (PF4)/CXCL4. Here, we show that the intra-α-granular proteoglycan, serglycin (SRGN), plays a key role in this process by retaining PF4, and perhaps other factors, during MK maturation. Immature, SRGN$^{-/-}$ MKs released ~80% of their PF4, and conditioned media from these cells negatively affected wild-type MK differentiation in vitro. This was replicated in wild-type MKs by treatment with the polycation surfen, a known inhibitor of glycosaminoglycan (GAG)/protein interactions. In vivo, SRGN$^{-/-}$ mice had an interstitial accumulation of PF4, transforming growth factor β1, interleukin-1β, and tumor necrosis factor α in their bone marrow and increased numbers of immature MKs, consistent with their mild thrombocytopenia. SRGN$^{-/-}$ mice also had reduced numbers of hematopoietic stem cells and multipotent progenitors, reduced laminin, and increased collagen I deposition. These findings demonstrate that MKs depend on SRGN and its charged GAGs to balance the distribution of PF4 and perhaps other factors between their α-granules and their adjacent extracellular spaces. Disrupting this balance negatively affects MK development and bone marrow microenvironment homeostasis.

Introduction

Megakaryocytes (MKs) are large polyploid cells predominantly residing within the bone marrow, where they produce platelets. MKs synthesize granules and other cellular components found in platelets, with α-granules being the most abundant granule type and containing the widest variety of biomolecules. MKs source α-granule content via de novo synthesis and endocytosis from their microenvironment.[1,2] These proteins are sorted within multivesicular bodies before being stored in granules. Recent studies have demonstrated how MKs affect bone marrow microenvironments via releasing factors such as platelet factor 4 (PF4)/CXCL4, transforming growth factor β1, and other extracellular matrix proteins, which contribute to the hematopoietic stem cell (HSC) niche and bone marrow fibrosis.[3-11] Through their secretory nature, MKs are unique players in homeostatic maintenance of local HSCs and their regulated expansion and differentiation; however, the mechanisms of this role have not been fully explored.[12,13]

Submitted 22 February 2024; accepted 17 June 2024; prepublished online on *Blood Advances* First Edition 28 June 2024. https://doi.org/10.1182/bloodadvances.2024012995.

Original data are available on request from the corresponding author, Sidney W. Whiteheart (whitehe@uky.edu).

The full-text version of this article contains a data supplement.

PF4 is one of the most abundant α-granule proteins.[14,15] Although PF4 is primarily expressed by MKs and found in platelets, some immune cells can express PF4 under inflammatory conditions that contribute to fibrosis.[16] PF4 is both released and endocytosed by MKs.[9,17-19] In the bone marrow, PF4 significantly affects HSC differentiation and MK development. High PF4 levels suppress MK maturation and HSC expansion,[18,19] and increased PF4 levels are associated with inflammation and marrow fibrosis in mice.[20,21] Conversely, low PF4 contributes to rapid exhaustion of HSC pools, affecting multiple hematopoietic cell lineages, including MKs.[9,18,22] Despite these clear effects, the mechanisms by which MKs maintain a balance between PF4 release and retention are unknown.

Supporting earlier observations,[23] our previous data demonstrated that PF4 interacts strongly with the α-granular proteoglycan, serglycin (SRGN).[24] SRGN is a major proteoglycan in endothelial and hematopoietic cells, especially MKs, found within granules and secretory vesicles.[25,26] It appears to be involved in hematopoietic cell differentiation, chemokine secretion, lymphoid cell activation, cytotoxic granule maturation, neutrophil granule formation, as well as tumor growth, metastasis, and angiogenesis.[27-30] It interacts with small positively charged proteins via its polyanionic, sulfated glycosaminoglycan (GAG) chains, which decorate the relatively small (18 kDa) polypeptide.[31] These GAGs and their sulfation patterns vary by cell type.[32,33] The PF4-SRGN interaction is due to electrostatic interactions between the sulfated glycans on SRGN and a ring of positively charged residues on the surface of PF4, similar to the interaction between PF4 and heparin.[34] Previous reports demonstrated defective platelet aggregation and thrombosis in SRGN$^{-/-}$ mice.[35] SRGN$^{-/-}$ mice presented with decreased platelet counts (780.33 thousand platelets/μL), and platelets from these mice contained 899.38 thousand platelets/μL of the PF4 pool found in wild-type platelets. In our studies, SRGN$^{-/-}$ MKs secreted significantly more PF4 than control MKs,[24] leading us to hypothesize that PF4's absence from SRGN$^{-/-}$ platelets was due to defective retention.

To investigate how SRGN affects PF4 trafficking, we examined MKs from SRGN$^{-/-}$ mice. We assessed how they retained PF4 during development and how defects in this affected marrow microenvironments. Neurobeachin-like 2 (NBEAL2)$^{-/-}$ MKs, which have a known defect in α-granule biogenesis, were used for comparison.[36-38] SRGN$^{-/-}$ and NBEAL2$^{-/-}$ MKs failed to retain PF4 during the early stages of development. Consistently, SRGN$^{-/-}$ bone marrow contained higher concentrations of PF4 in the interstitial fluid. SRGN$^{-/-}$ MKs were smaller and more immature than wild-type, and bone marrow morphology was altered, with decreased laminin and increased collagen I levels. SRGN deficiency decreased the number of marrow HSCs as well as multipotent progenitors. In summary, we show the important mechanism by which SRGN regulates PF4 retention during MK maturation, thus influencing homeostasis of the HSC niche.

Methods

Bone marrow and BMW isolation

Bone marrow was isolated from mouse long bones (12-25 weeks), unless otherwise noted, by centrifugation of cut bones held in a 200-μL tube with the bottom cut open and nested within a 1.5-mL tube as described.[39] These tubes were subjected to 2500*g* for 40 seconds, and cells were resuspended in the appropriate media.

Bone marrow wash (BMW) was isolated by adding 50 μL of RPMI-1640 (Fisher Scientific; catalog no. 11-875-093) to a 1.5-mL tube before spinning. After marrow isolation, the cells were centrifuged again at 200*g* for 5 minutes, and the supernatant was collected and centrifuged once more at 17 000*g* for 10 minutes.

Cryosectioning and immunostainings

Femurs harvested from SRGN$^{-/-}$, NBEAL2$^{-/-}$, or wild-type mice were fixed in 4% (wt/vol) paraformaldehyde in phosphate-buffered saline (PBS) for 24 hours at 4°C, after which they were transferred into 10% (wt/vol) sucrose in PBS. A sucrose gradient was performed, and femurs were embedded in a water-soluble embedding medium, then frozen, and sectioned at 10 μm on a cryostat (Leica Biosystems).[40] After rehydration in PBS, sections were blocked using 10% (vol/vol) donkey serum and stained for CD41 (BioLegend; catalog no. 133902), laminin (Sigma-Aldrich; catalog no. L9393), and PF4 (Invitrogen; catalog no. MA5-38089) overnight at 4°C. Secondary antibodies were from Invitrogen. Slides were stained with 4′,6-diamidino-2-phenylindole, washed, and mounted using Fluoroshield mounting medium (Sigma-Aldrich; catalog no. F6182). Images were acquired at a Zeiss LSM880 microscope (20× objective). Whole sections were imaged (BioTek Lionheart; 4× objective), and MK numbers were quantified using an automated imaging platform. Analysis of fluorescence intensity was performed using ZEISS ZEN Blue version 3.8 (Carl Zeiss Microscopy) by measuring channel-specific intensity across entire sections after background subtraction.

Flow cytometry on bone marrow–derived MKs and progenitors

Femurs, tibias, and iliac crests were harvested from SRGN$^{-/-}$, NBEAL2$^{-/-}$, or wild-type mice and processed as previously described.[41] Briefly, marrow was retrieved by centrifugation at 2500*g* for 40 seconds into 100 μL of PBS. Red blood cells were lysed using activated Cdc42-associated kinase buffer (Thermo Fisher; catalog no. A1049201) for 5 minutes at room temperature. Cells were filtered through a 70-μm cell strainer. Single-cell suspensions were stained on ice for 30 minutes and analyzed using spectral flow cytometry (Cytek Aurora 4 laser system). Data were analyzed using the Diva software (BD Biosciences) and FlowJo (Tree Star Inc). All antibodies were acquired from BioLegend. Cell populations were defined as follows: mature MKs as CD45$^+$Lin$^-$Cd41$^+$CD42d$^+$; MK progenitors as CD45$^+$Lin$^-$Sca-1$^-$c-Kit$^+$CD150$^+$CD41$^+$; long-term HSCs as CD45$^+$Lin$^-$Sca-1$^+$c-Kit$^+$Flt3$^-$CD150$^+$CD48$^-$; short-term HSCs as CD45$^+$Lin$^-$Sca-1$^+$cKit$^+$Flt3$^-$CD150$^-$CD48$^-$; MPP4 as CD45$^+$Lin$^-$Sca-1$^+$c-Kit$^+$Flt3$^+$; MPP3 as CD45$^+$Lin$^-$Sca-1$^+$c-Kit$^+$Flt3$^-$CD150$^-$CD48$^+$; and MPP2 as CD45$^+$Lin$^-$Sca-1$^+$c-Kit$^+$Flt3$^-$CD150$^+$CD48$^+$.

Statistical analysis

Statistical analysis was performed using GraphPad Prism version 10.0.0 for Windows (GraphPad Software, Boston, MA; www.graphpad.com). Comparisons between 2 groups were performed using unpaired *t* test or Mann-Whitney test. Comparisons between >3 groups were performed using ordinary 1-way analysis of variance, followed by Dunnett multiple comparisons test or Kruskal-Wallis test, followed by Dunn multiple comparisons test. Significance was set at the following: not significant (ns) is indicated by

$P > .05$; *$P \leq .05$; **$P \leq .01$; ***$P \leq .001$; ****$P \leq .0001$. All error bars represent the standard error of the mean.

All animal work was approved by the institutional animal care and use committee at the University of Kentucky (protocol number 2019-3384). Human samples and participants were not used in this study.

Additional methods are provided in supplemental Information.

Results:

PF4 release is increased in SRGN$^{-/-}$ and NBEAL2$^{-/-}$ bone marrow

To investigate the reduced PF4 levels in SRGN$^{-/-}$ MKs,[24] we compared SRGN$^{-/-}$ mice with another model of defective α-granule biogenesis, NBEAL2$^{-/-}$. In NBEAL2$^{-/-}$ MKs, α-granule cargo colocalizes with Rab11^{+} compartments before being released.[36] This led us to hypothesize that PF4 and other soluble α-granule proteins may similarly be released into the extracellular space within the bone marrow of these mice. We assessed multiple cytokines in BMW samples (Figure 1). We detected a significant increase in PF4 in both SRGN$^{-/-}$ and NBEAL2$^{-/-}$(Figure 1A), despite a decrease in PF4 messenger RNA (mRNA) in both (supplemental Figure 1A). PF4 mRNA expression increases at later stages of MK maturation because FLI-1 and GATA-1 bind and activate its promoter,[42,43] so decreased PF4 mRNA levels may be indicative of suppressed MK maturation. PF4 in wild-type and NBEAL2$^{-/-}$ BMWs was complexed with SRGN (supplemental Figure 1B), and increased PF4 release was confirmed in vitro (supplemental Figure 1C), consistent with our previous findings.[24] Additionally, in vitro–derived SRGN$^{-/-}$ MKs were smaller than wild-type, again indicating potential defects in their maturation (Supplemental Figure 1D-E).

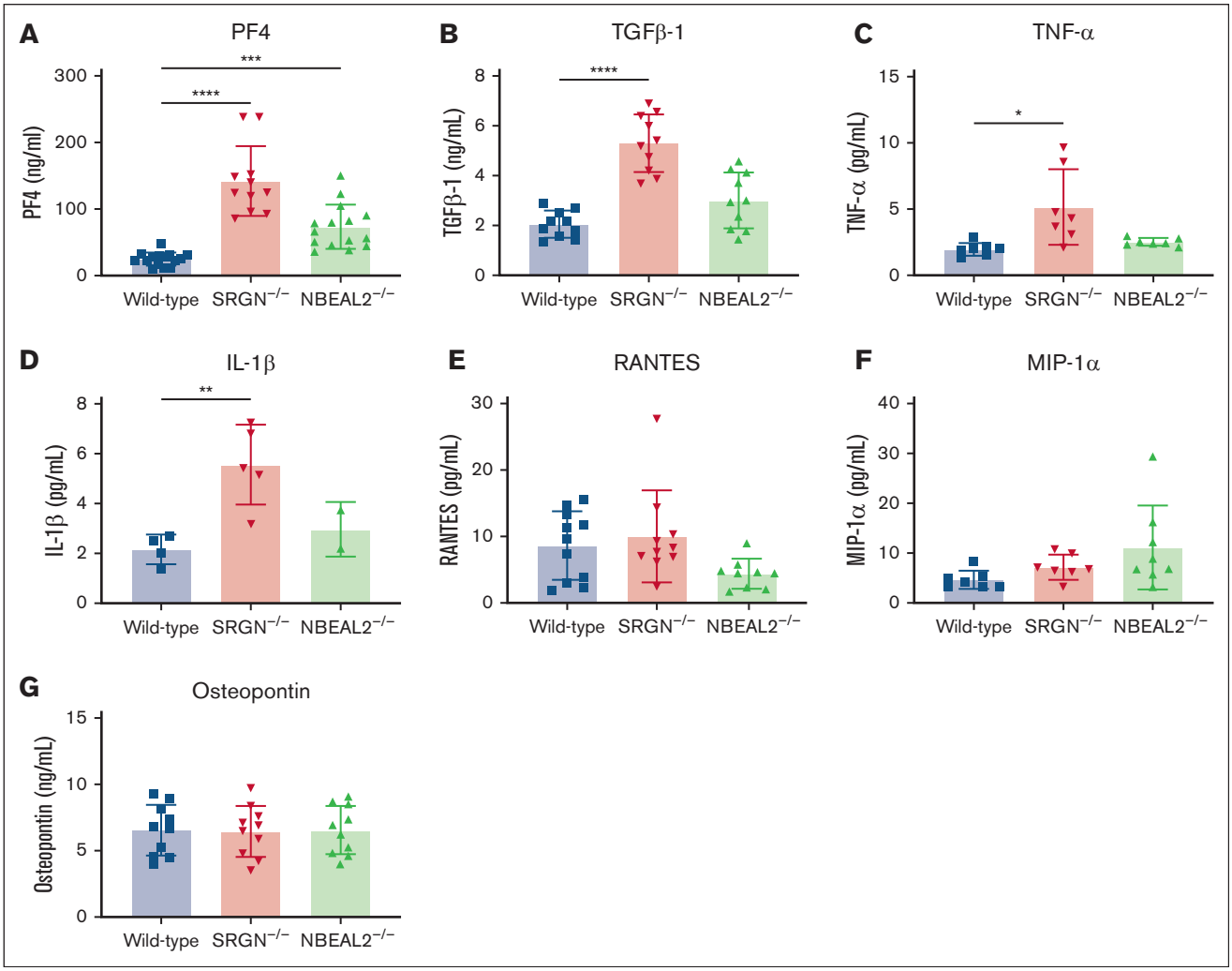

Figure 1. Extracellular cytokine levels are increased in SRGN$^{-/-}$ bone marrow. (A-G) Concentration of PF4 (wild-type [WT], n = 15; SRGN$^{-/-}$, n = 11; NBEAL2$^{-/-}$, n = 15) (A); TGF-β1 (n = 10) (B); TNF-α (n = 7) (C); IL-1β (n = 7) (D); RANTES (WT, n = 11; SRGN$^{-/-}$, n = 10; NBEAL2$^{-/-}$, n = 9) (E); MIP-1α (n = 7) (F); and osteopontin (n = 1; G) in BMWs from adult mice. Each point represents the average of 2 technical replicates from a single mouse. Significance: ns is indicated by $P > .05$; *$P \leq .05$; **$P \leq .01$; ***$P \leq .001$; ****$P \leq .0001$. All error bars represent the standard error of the mean (SEM). IL-1β, interleukin-1β; MIP-1α, macrophage inflammatory protein-1 alpha; ns, not significant; RANTES, regulated on activation, normal T cell expressed and secreted/CCL5; TGF-β1, transformation growth factor β1; TNF-α, tumor necrosis factor α.

Additionally, we found significant increases in transforming growth factor β1, tumor necrosis factor α, and interleukin-1β in SRGN$^{-/-}$ BMWs, whereas RANTES, macrophage inflammatory protein-1α, and osteopontin were unchanged (Figure 1B-G). The increased cytokine levels indicate that the SRGN$^{-/-}$ bone marrow environment is proinflammatory and potentially inhospitable to normal megakaryopoiesis, representing a potential feedback mechanism that could control function. It should be noted that these factors are not derived exclusively from MKs, and thus, these changes may be due to release from other cell types. To directly evaluate the role of MKs in this process, we further examined the specific release of PF4 because its expression is MK specific, and thus, it is an indicator of their actions.

PF4 is not targeted to a degradative compartment by loss of SRGN or NBEAL2

Defects in α-granule protein trafficking could lead to mistargeting of the proteins to degradative compartments and thus their reduction.[44,45] We tested the degradation of PF4 in SRGN$^{-/-}$ and NBEAL2$^{-/-}$ MKs using bafilomycin A1 treatment. Bafilomycin A1 prevents the degradation of mistargeted proteins in many cell types, including MKs,[44,45] but did not rescue the intracellular PF4 levels in SRGN$^{-/-}$ or NBEAL2$^{-/-}$ MKs. For NBEAL2$^{-/-}$ MKs, PF4 levels did increase over 4 hours but did not reach wild-type levels (Figure 2A-B). These results were validated by western blotting (supplemental Figures 2 and 3), confirming that both SRGN and NBEAL2 are necessary for PF4 retention, potentially in RAB11^{+} recycling endosomes, because they serve as a primary sorting endosome for α-granule cargo.[44,45] Based on our results and the literature, we propose that PF4 is not sufficiently retained in this compartment in the absence of SRGN or NBEAL2 for proper sorting to occur. Instead, the most PF4 is released via normal exchange between this compartment and the plasma membrane.

SRGN$^{-/-}$ and NBEAL2$^{-/-}$ MKs release PF4 earlier in development than wild-type MKs

In supplemental Figure 1, PF4 mRNA expression is suppressed in SRGN$^{-/-}$ and NBEAL2$^{-/-}$ MKs despite its greater release in BMWs. Given that PF4 expression is linked to 2 transcription factors that increase as MKs mature (FLI-1 and GATA-1), we investigated PF4 expression and distribution during MK development using lineage-depleted cultures (Figure 2). We observed an increase in PF4 mRNA during differentiation that was 10-fold higher than that seen in SRGN$^{-/-}$ and NBEAL2$^{-/-}$ MKs (Figure 2C). SRGN mRNA expression was constant in wild-type MKs, whereas NBEAL2$^{-/-}$ MKs had lower SRGN expression on days 1 to 3 but reached wild-type levels by day 5 (Figure 2D). Total PF4 (the sum of intracellular and media PF4) was similar until day 5, when it increased in wild-type MKs but not in the SRGN$^{-/-}$ or NBEAL2$^{-/-}$ MKs (Figure 2E). Because *PF4* gene expression peaks at later stages of MK development, the paradox surrounding increased PF4 release in the bone marrow coupled with decreased PF4 mRNA (Figure 1; supplemental Figure 1) might be explained by the fact that SRGN$^{-/-}$ and NBEAL2$^{-/-}$ MKs do not reach full maturity.[42,43] Because developing MKs express PF4, the immature MKs could be the source of released PF4 in the cultures of the SRGN$^{-/-}$ and NBEAL2$^{-/-}$ MKs. Consistently, immature wild-type MKs (days 1-3) accumulated intracellular PF4 during the first 3 days of culture, whereas SRGN$^{-/-}$ and NBEAL2$^{-/-}$ MKs did not (Figure 2F). Instead, there was an increase in secreted PF4 during the earlier stages of MK development of the SRGN$^{-/-}$ and NBEAL2$^{-/-}$ cells (Figure 2G). Only 20% of the PF4 in the wild-type cultures was in the medium, which increased to ~40% by day 5 (Figure 2H). In cultures of the knockout MKs, >80% of the total PF4 pool was found in the media at day 2 and that remained elevated (Figure 2H). We posit that the difference in PF4 distribution is a consequence of the inability of SRGN$^{-/-}$ and NBEAL2$^{-/-}$ MKs to retain PF4. This could be due to faulty retention during biosynthesis or a lack of endocytosis and/or retention once PF4 is constitutively secreted. In either case, our results suggest that the balance between retention and release is modulated by SRGN as MKs mature. The lack of change in SRGN mRNA expression between days 2 and 5 in wild-type MKs (Figure 2C) suggests that the stage-dependent, increased PF4 expression (Figure 2B) overcomes SRGN levels and accounts for the increased release of PF4 at later stages.

MK maturation is suppressed by SRGN$^{-/-}$ conditioned media or a GAG inhibitor

Our results demonstrate a potential mechanism by which MKs increase extracellular PF4 and thus regulate the maturation of their neighbor MKs, a known effect of PF4.[17,18] PF4 regulates multiple other processes in the bone marrow, such as HSC quiescence, fibrosis, and immune cell activation.[7,9,16,21,22] High PF4 restricts the development of immature MKs and regulates HSC quiescence.[9,19,22] To investigate this, we performed a conditioned media experiment exchanging the media of wild-type and SRGN$^{-/-}$ MK cultures. Wild-type cells grown in SRGN$^{-/-}$ conditioned media showed decreased levels of CD41 and CD42b (Figure 3A) and had fewer high-ploidy (8N-16N) MKs and an increase in the lower-ploidy (2N-4N) populations (Figure 3B). SRGN$^{-/-}$ MKs grown under all conditions exhibited lower CD41 and CD42b (Figure 3A), and their MK populations were skewed toward lower-ploidy populations (Figure 3B). These findings suggest that the in vitro growth defect observed in SRGN$^{-/-}$ MKs is due to soluble factors released by SRGN$^{-/-}$ MKs. Based on our data and the literature, PF4 is a likely contributor to this phenotype, although almost certainly not the only one.

To address the effects of PF4 on MK development, we added recombinant PF4 (50 ng/mL) to differentiating MKs on day 3 to reach similar concentrations found in SRGN$^{-/-}$ conditioned media (Figure 3C-D). We observed similar decreases in CD41 and CD42b levels (Figure 3C) as those seen with SRGN$^{-/-}$ conditioned media, along with similar shifts toward lower-ploidy stages with PF4 treatment (Figure 3D). PF4 treatment did not exacerbate these phenotypes in SRGN$^{-/-}$ MKs.

To further define this effect, we used the GAG competitive inhibitor, surfen, a small polycation that binds GAG chains with high affinity and, via competition, displaces GAG binding partners.[46] We hypothesized that treatment of developing MKs with surfen would phenocopy the lack of SRGN and cause PF4 release. The intracellular pool of PF4 decreased in wild-type MKs based on immunofluorescence experiments and western blot (Figure 4A-D). Wild-type MKs treated with surfen over 4 hours released PF4, similar to what was seen with SRGN$^{-/-}$ MKs (Figure 4E). These results show that surfen treatment mimicked the PF4 release phenotype observed in SRGN$^{-/-}$ MKs. We next determined

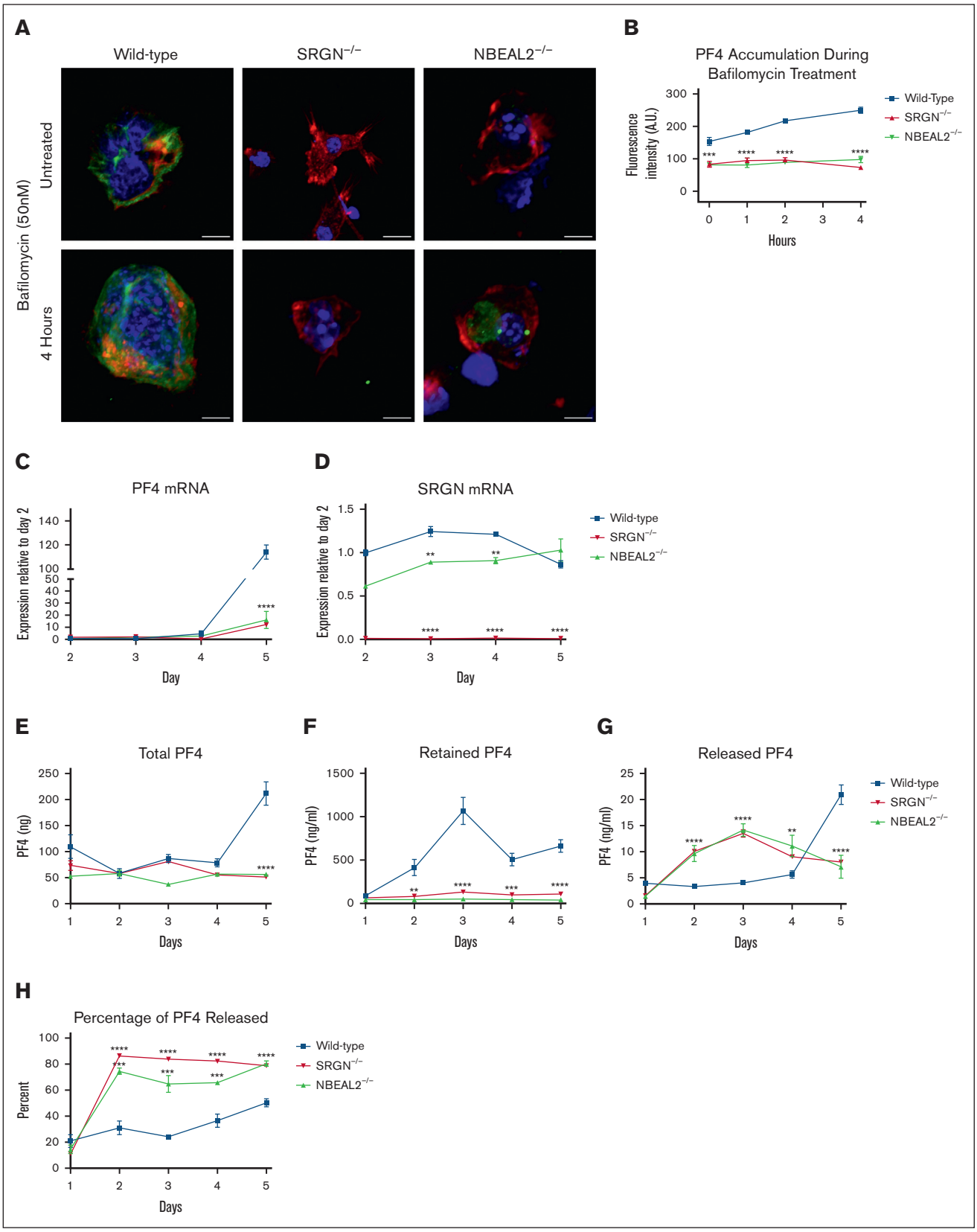

Figure 2. SRGN$^{-/-}$ and NBEAL2$^{-/-}$ MKs fail to retain PF4 at early stages of development. (A) Representative maximum intensity projection images of isolated, mature (day 5) MKs adhered to fibrinogen-coated slips overnight and treated with bafilomycin (50 nM) for 4 hours. Actin (red), DAPI (4′,6-diamidino-2-phenylindole)/DNA (blue), and PF4 (green). The scale bar represents 10 μm. (B) Quantification of PF4 fluorescence intensity normalized to background fluorescence within each image. Data represent an average of

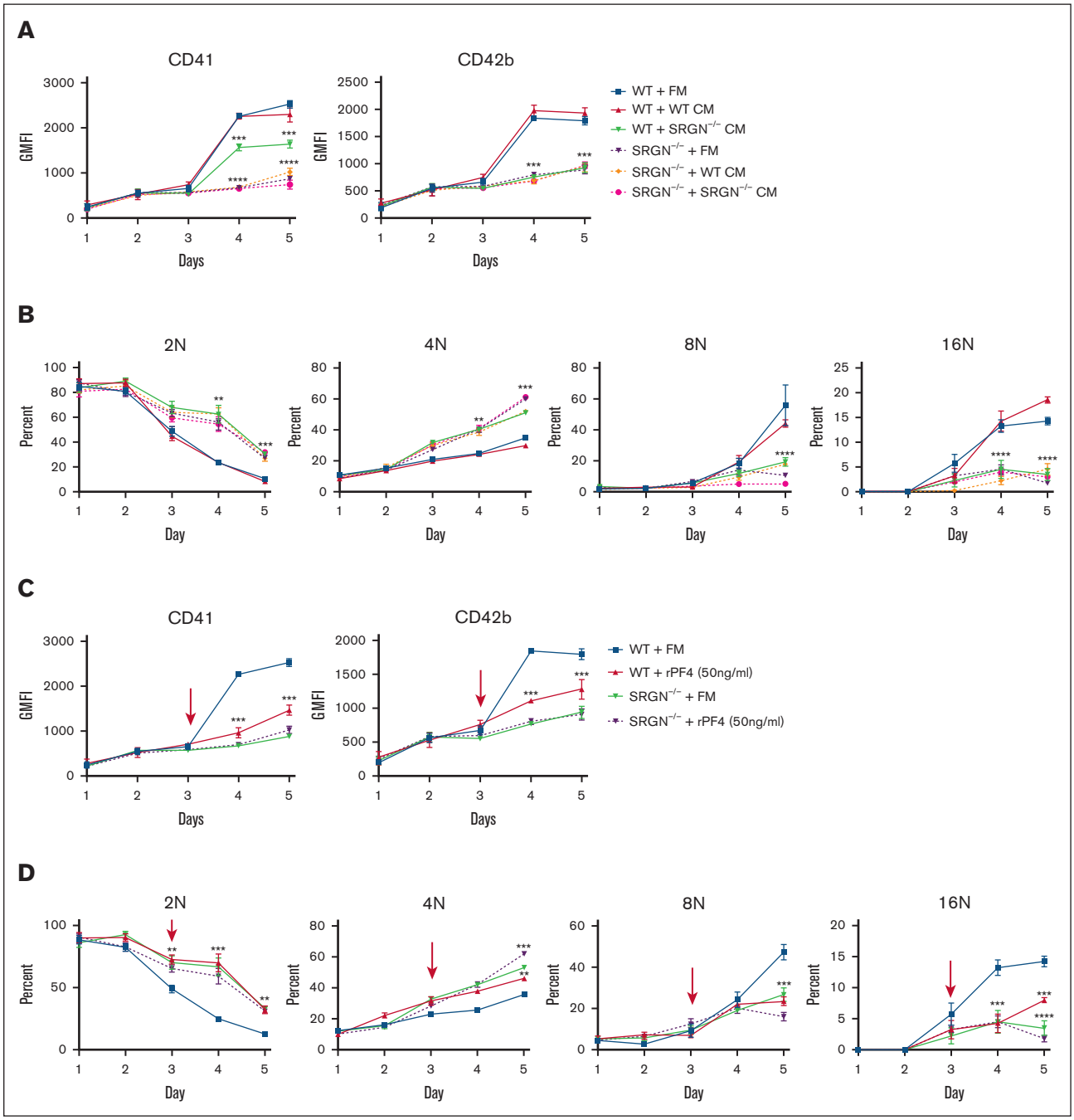

Figure 3. MK development is restricted by SRGN$^{-/-}$ conditioned media and PF4 in vitro. (A) Geometric mean fluorescence intensity (GMFI) of CD41 and CD42b staining of MKs during differentiation in either fresh media (FM), WT conditioned media (CM), or SRGN$^{-/-}$ CM; n = 5. (B) The percentage of the total single-cell population collected residing with either the 2N, 4N, 8N, or 16N peak after propidium iodide staining; N = 5. (C) GMFI of CD41 and CD42b staining of MKs during differentiation in either FM or media supplemented with 50 ng/mL rPF4 on day 3. The arrow indicates treatment time point; n = 5. (D) The percentage of the total single-cell population collected residing with either the 2N, 4N, 8N, or 16N peak after propidium iodide staining; n = 5. Significance was determined by comparing each group with the corresponding WT with FM treatment. Significance: ns is indicated by $P > .05$; *$P \leq .05$; **$P \leq .01$; ***$P \leq .001$; ****$P \leq .0001$. All error bars represent the SEM. rPF4, recombinant platelet factor 4.

Figure 2 (continued) 15 individual cells from each time point. (C) PF4 mRNA during MK differentiation from lineage-depleted cells. Shown as a ratio to WT day 2 average; n = 4. (D) SRGN mRNA during MK differentiation from lineage-depleted cells. Shown as a ratio to WT day 2 average; n = 2. (E) Total PF4 production in lineage-depleted MK cultures until day 5, determined by the addition of the total mass of PF4 in the lysate and media. PF4 concentrations in each fraction were measured by enzyme-linked immunosorbent assay (ELISA), and mass was calculated based on volume; n = 5. (F) Retained PF4 concentrations, determined from lysate fraction as described in panel E; n = 5. (G) Released PF4 concentrations, determined from media fraction as described in panel E; n = 5. (H) Data show the percentage of total PF4 mass (E) found in the media (G) throughout the experiment. Data represent an average of 5 independent experiments. All significance is relative to the corresponding WT time point. Significance: ns is indicated by $P > .05$; *$P \leq .05$; **$P \leq .01$; ***$P \leq .001$; ****$P \leq .0001$. All error bars represent the SEM.

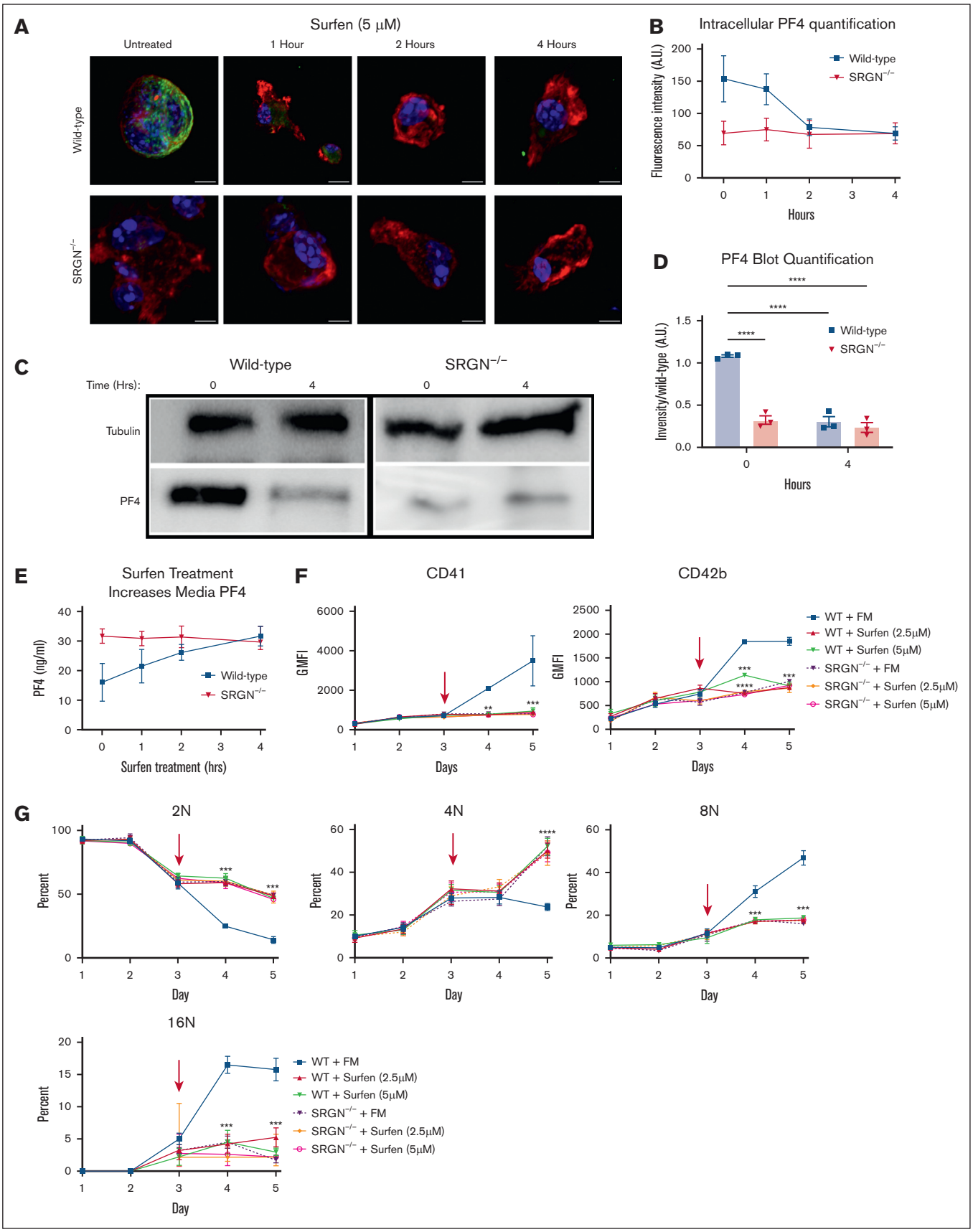
A
Surfen (5 μM)
Untreated
1 Hour
2 Hours
4 Hours
Wild-type
SRGN−/−
B
Intracellular PF4 quantification
Fluorescence intensity (A.U.)
Wild-type
SRGN−/−
Hours
C
Wild-type
SRGN−/−
Time (Hrs):
Tubulin
PF4
D
PF4 Blot Quantification
Invensity/wild-type (A.U.)
Hours
E
Surfen Treatment Increases Media PF4
PF4 (ng/ml)
Surfen treatment (hrs)
F
CD41
CD42b
GMFI
Days
WT + FM
WT + Surfen (2.5μM)
WT + Surfen (5μM)
SRGN−/− + FM
SRGN−/− + Surfen (2.5μM)
SRGN−/− + Surfen (5μM)
G
2N
4N
8N
16N
Percent
Day

Figure 4.

whether surfen treatment also suppressed MK development because it increased extracellular PF4. In wild-type cells, surfen treatment lowered CD41 and CD42b levels (Figure 4F) and decreased high-ploidy (8N-16N) populations in the cultures (Figure 4G). No significant effects were observed when SRGN$^{-/-}$ cells were treated with surfen, as expected, suggesting no off-target effects of the compound.[24] These findings collectively show that SRGN-PF4 ionic interactions are necessary for PF4 retention, and disruption of this interaction leads to the accumulation of PF4 in the media and a blunting of MK maturation.

MK development is suppressed in SRGN$^{-/-}$ mice

We sought to determine whether the phenotypes observed in vitro were manifested in the bone marrow niche in vivo. Given that increased PF4 has been associated with impaired HSC quiescence and marrow fibrosis,[20,21,47,48] we speculated that SRGN$^{-/-}$ mice would develop fibrosis or similar phenotypes with age. Platelet counts of 52-week-old mice were significantly decreased in SRGN$^{-/-}$ mice, consistent with our previous findings (Figure 5A),[24] whereas there was no change in mean platelet volume (Figure 5B). All other circulating blood cell counts were normal except for an increase in circulating lymphocytes and total white blood cells (supplemental Figure 4). We found no significant change in the number of CD41^{+}/CD42b^{+} cells in the bone marrow, but when the ploidy of this population was assessed, we found a significant skewing of the SRGN$^{-/-}$ populations toward the lower stage (4N) and away from the higher stages (8N-16N; Figure 5D). Moreover, SRGN$^{-/-}$ mice exhibited decreased MK-primed progenitor cells (CD45^{+}Lin^{-}Sca-1^{-}c-Kit^{+}CD150^{+}CD41^{+}) and MKs (CD45^{+}Lin^{-}CD41^{+}CD42d^{+}; Figure 5E-F). Consistently, the number of MK colony-forming units was decreased from SRGN$^{-/-}$ bone marrow (Figure 5G). Defective megakaryopoiesis or MK differentiation likely contributes to the decreased platelet count and the altered HSC niche, which rely on the release of local cytokines from MKs.[4,11,13,22]

SRGN$^{-/-}$ bone marrow morphology and HSCs are disrupted

We observed a decrease in average MK size in SRGN$^{-/-}$ mice (Figure 6A-B), consistent with our findings that MK ploidy and size were both decreased in culture and young marrow. This was confirmed via CD41-DAB and hematoxylin and eosin staining of bone sections (supplemental Figure 5). PF4 was increased, whereas laminin deposition decreased in SRGN$^{-/-}$ mice (Figure 6C-D). There is a strong association between PF4 and the development of fibrosis in multiple tissues.[16,20,21] Consistently, we detected more collagen I in SRGN$^{-/-}$ mice (Figure 6E-F), suggesting a fibrotic environment.[49] This fibrosis is potentially driven by excessive levels of PF4, but other factors shown to be increased in SRGN$^{-/-}$ marrow (Figure 1) could contribute to the phenotype. These increases are likely due to a combination of MK release and release from other cell types. We also investigated the HSC populations in SRGN$^{-/-}$ marrow and observed reductions in multipotent progenitor populations (MPPs) 2, 3, and 4 (Figure 7A-C). Similar to these results and to previous studies showing increased HSC proliferation upon decreased PF4 release,[9,22] we found decreased numbers of both short- and long-term HSCs in SRGN$^{-/-}$ marrow (Figure 7D-E). There were no changes in other cell populations (supplemental Figure 6). Taken together, these results suggest that loss of SRGN disrupts the balance of MKs release/retention, which is essential for the maintenance of HSC populations and MPPs.

Discussion

This work adds to the growing understanding of MKs' role in marrow microenvironments. We demonstrate that SRGN and NBEAL2 are necessary for the retention of PF4 by MKs during α-granule biogenesis. Loss of either leads to the release of PF4, which occurred in immature MKs. Wild-type MKs prioritized retention of PF4 in early stages, but fully mature MKs released PF4 as its mRNA expression increased. Likely, this is a paracrine mechanism by which mature MKs affect proximal MK precursors when mature MK numbers are sufficient. Others have reported how NBEAL2 is needed for the retention of α-granule proteins.[36] Our data confirm this for PF4. NBEAL2 is most likely involved in a general retention of many α-granule proteins through a yet uncharacterized mechanism. The similar release of PF4 in SRGN$^{-/-}$ and NBEAL2$^{-/-}$ MKs implies that both are key regulators of PF4 trafficking. Recent work has shown that recycling endosomes are the sorting nexus for many α-granule cargoes.[44,45] Granule cargoes, for example, PF4, localize to the recycling endosome after release from the Golgi, and it is in this compartment that PF4, fibrogen, von Willebrand factor, and other α-granule proteins are sorted and concentrated before moving to the multivesicular bodies.[44,45,50] Subsequent trafficking appears dependent on factors such as NBEAL2, SEC22B, syntaxin 12, VPS33B/16B, and COMMD3.[36,44,45,51]

PF4 release from MKs in the bone marrow was first described by Lambert et al[19] and since has been confirmed by others.[9,22,52] MKs also endocytose PF4 from their microenvironment.[17,18] This places MKs at the crossroads of PF4 regulation within the bone marrow. Deletion of SRGN or NBEAL2 disrupts this process and causes the release of some or all α-granule cargoes into the surrounding microenvironment. For SRGN, the most affected proteins are those that are positively charged and interact with polyanions, for example, PF4. Originally, in 1972, PF4 was purified in a complex with a chondroitin-4-sulfate proteoglycan from platelet releasates.[23] These early studies unknowingly characterized PF4-SRGN complexes before the discovery of SRGN. We now know that the

Figure 4. PF4 retention is inhibited by surfen and restricts MK development in vitro. (A) Representative maximum intensity projection images of isolated, mature (day 5) MKs adhered to fibrinogen-coated slips overnight and treated with surfen (5 μM) for 0, 1, 2, and 4 hours. Actin (red), DAPI/DNA (blue), and PF4 (green). The scale bar represents 10 μm. (B) Quantification of PF4 fluorescence intensity normalized to background fluorescence within each image. Data represent an average of 15 individual cells. (C) Western blots of PF4 in MK lysates at 0 and 4 hours of surfen (5 μM) treatment with tubulin as loading control. (D) Quantification of signal intensity from panel C. (E) Media PF4 concentrations during treatment of mature (day 5) MKs with surfen (5 μM) over 4 hours determined from media sample by ELISA; n = 4. (F) GMFI of CD41 and CD42b staining of MKs during differentiation in FM supplemented with 2.5 μM or 5 μM surfen on day 3. The arrow indicates treatment time point; n = 4. (G) The percentage of the total single-cell population collected residing with either the 2N, 4N, 8N, or 16N peak after propidium iodide staining; n = 5. Significance was determined by comparing each group with the corresponding WT with FM treatment. Significance: ns is indicated by $P > .05$; *$P \leq .05$; **$P \leq .01$; ***$P \leq .001$; ****$P \leq .0001$. All error bars represent the SEM.

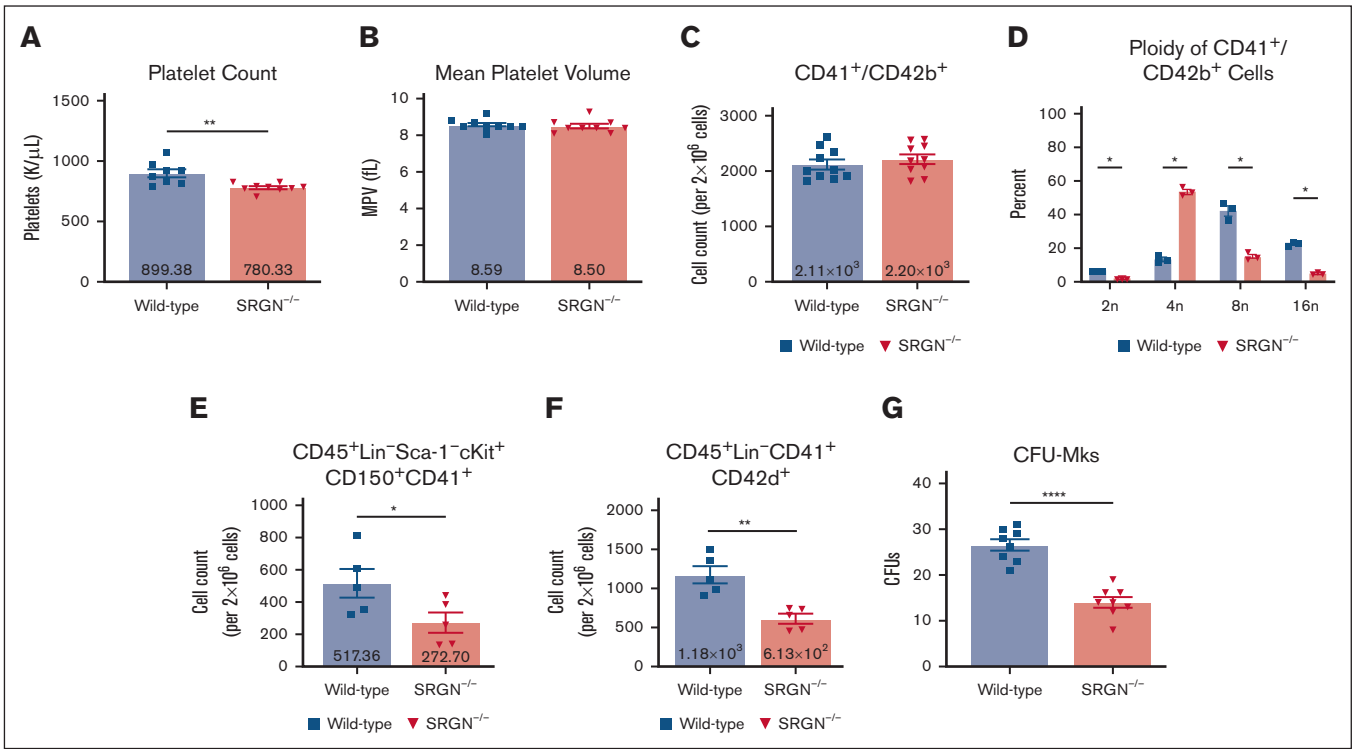

Figure 5. MK maturation and platelet count are suppressed in SRGN$^{-/-}$ mice. (A) Platelet count was determined by complete blood count from mice (WT, n = 8; SRGN$^{-/-}$, n = 9). (B) Mean platelet volume (WT, n = 8; SRGN$^{-/-}$, n = 9). (C) The number of CD41^{+}/CD42b^{+} bone marrow–derived cells; n = 10. (D) The percentage of CD41^{+}/CD42b^{+} cells that reside within the indicated ploidy peak after propidium iodide staining; n = 3. (E) CD45^{+}Lin^{-}CD41^{+}CD42d^{+} and (F) CD45^{+}Lin^{-}Sca-1^{-}c-Kit^{+}CD150^{+}CD41^{+} bone marrow cell counts as determined by flow cytometry (n = 5). (G) MK^{+} colonies produced from pooled bone marrow and assessed by acetylcholinesterase detection (n = 8). All experiments were performed with samples from 52-week-old mice. Significance: ns is indicated by $P > .05$; *$P \leq .05$; **$P \leq .01$; ***$P \leq .001$; ****$P \leq .0001$. All error bars represent the SEM. CFUs, colony-forming units. K/μL, thousands per microliter.

sulfated GAG chains on SRGN mediate interactions with many small, charged proteins simultaneously, acting as a large negatively charged "sponge." The regulatory effects of PF4 on MKs are clear, but the details of the receptor(s) involved and downstream signaling are unknown. The only described interaction between PF4 and an MK receptor is with LRP-1, in which it is necessary for PF4 signaling to affect MK development.[18] Thus more work is needed to determine whether free PF4 is the key regulator or whether SRGN-bound complexes play a role.

The alterations in MK progenitor and HSC populations noted in SRGN$^{-/-}$ mice coincides with recent discoveries, demonstrating the importance of MK cytokine secretion on hematopoietic niches.[5,7,9,11,22] In Figure 7, elevated PF4 levels correlated with reduced HSC populations. We speculate that the loss of SRGN may precipitate feedback impairing lymphoid differentiation, which promotes bone marrow fibrosis and is not conducive for HSC/MPP proliferation and maintenance (Figure 6) or development of MK progenitors (Figure 5). The mechanism by which SRGN directly influences HSC homeostasis is unclear, but HSCs are known to reside proximal to MKs.[7] This unique niche promotes the maintenance of HSCs and MPPs that are primed for MK and platelet production.[53,54] HSCs of these niches share many similar surface receptor and gene expression phenotypes with MKs, potentially explaining their similar responses to agonists such as thrombopoietin and PF4.[52,55-60] Beyond direct signaling from PF4 onto HSCs, increased PF4 levels may further alter the microenvironment, reducing laminin, an important component of this niche,[61-64] disrupting bone marrow homeostasis via fibrosis. Of note, MK proliferation and maturation were reduced in suspension cultures of SRGN$^{-/-}$ MKs, which had high PF4 concentrations (Figures 3 and 4). Thus, the restricted MK maturation in vivo is not exclusively the result of extracellular matrix alterations and is influenced by soluble factors. The alterations in HSC populations in SRGN$^{-/-}$ marrow did not precipitate changes in other circulating blood cells beyond platelets and lymphocytes. This could be due to compensatory repopulation of these lineages by the other multipotent progenitor cells.[53] We suspect that a systemic challenge to SRGN$^{-/-}$ mice (ie, sepsis) may expose a defect in their hematopoietic potential.

The effects on bone marrow homeostasis in SRGN$^{-/-}$ mice are likely not solely due to MK-derived SRGN because it is expressed by all hematopoietic cells and some nonhematopoietic cells, for example, endothelial cells.[33,65,66] The loss of SRGN from any of these could negatively affect their functions and properties. However, decreased HSCs and altered extracellular matrix is evidence that SRGN has key roles in the maintenance of niche microenvironment. Proteoglycans often function as concentrating factors that raise the local availability of specific growth factors and signaling proteins by retaining them or shielding them from degradation.[67-69] SRGN expression positively correlates with the development of multiple hematological malignancies, for example, leukemia, and cancer metastasis, in which it has been a biomarker

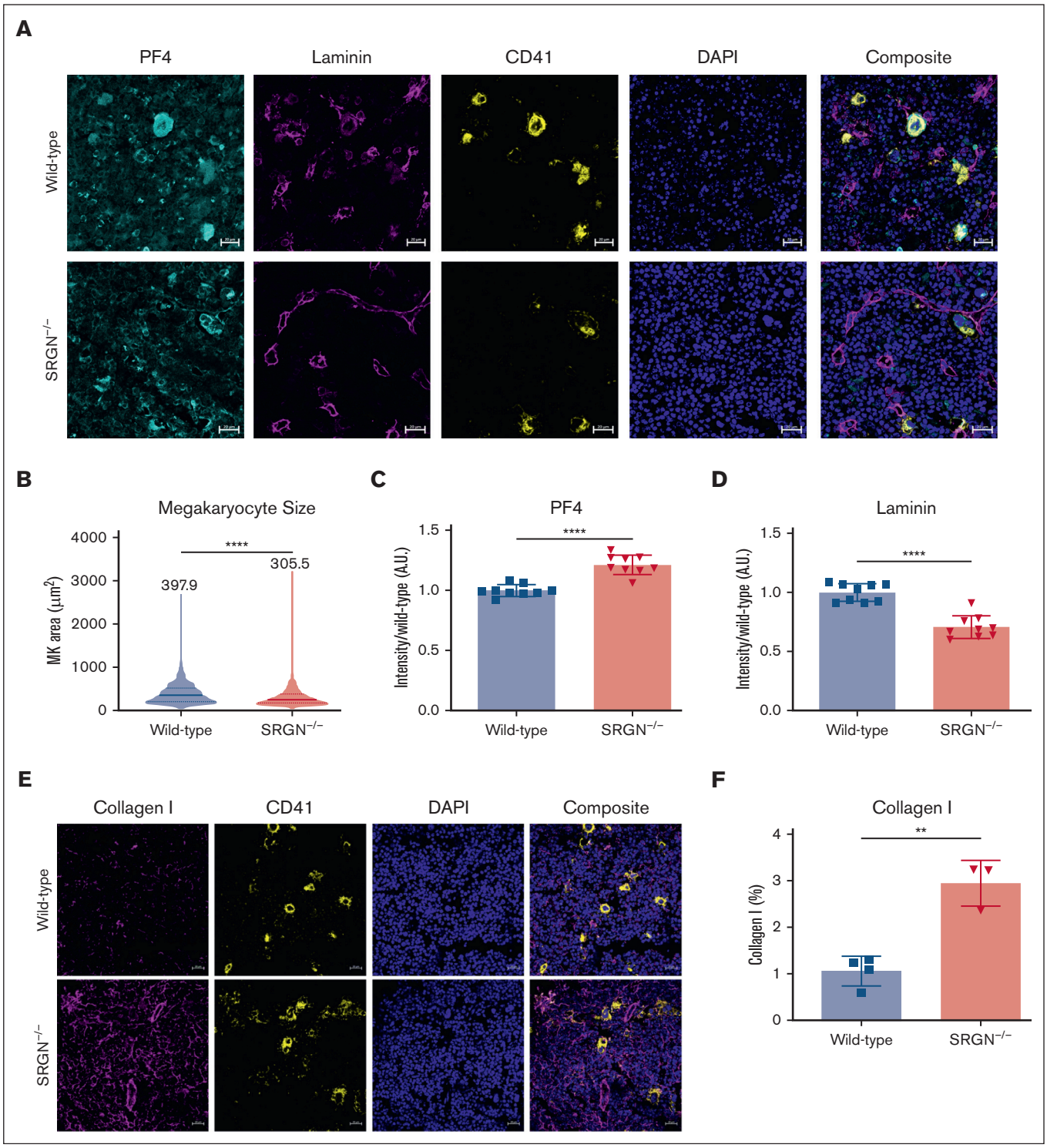

Figure 6. SRGN$^{-/-}$ mice have smaller MKs, increased PF4, and altered basement membrane protein levels. (A) Representative images of femur bone marrow from mice (aged 52 weeks). PF4 (cyan), Laminin (purple), CD41 (yellow), and DAPI (blue). The scale bar represents 20 μm. (B) MK size as determined by the size of CD41 stained cells. Bones from 9 individual mice were evaluated per group. The data shown are representative of the distribution of individual cell areas from each animal (WT, n = 2050; SRGN$^{-/-}$, n = 2901). (C) Quantification of PF4 fluorescence intensity normalized to background fluorescence within each image and displayed as a ratio to WT average intensity. Each point represents an individual mouse (n = 9). (D) Quantification of laminin fluorescence intensity normalized to background fluorescence within each image and displayed as a ratio to WT average intensity. Each point represents an individual mouse (n = 9). (E) Representative images of femur bone marrow from mice (aged 52 weeks). Collagen I (purple), CD41 (yellow), and DAPI (blue). The scale bar represents 20 μm. (F) Quantification of collagen I–positive area within each image in panel F. Each point represents an individual mouse (n = 9). Significance: ns is indicated by $P > .05$; *$P \leq .05$; **$P \leq .01$; ***$P \leq .001$; ****$P \leq .0001$. All error bars represent the SEM.

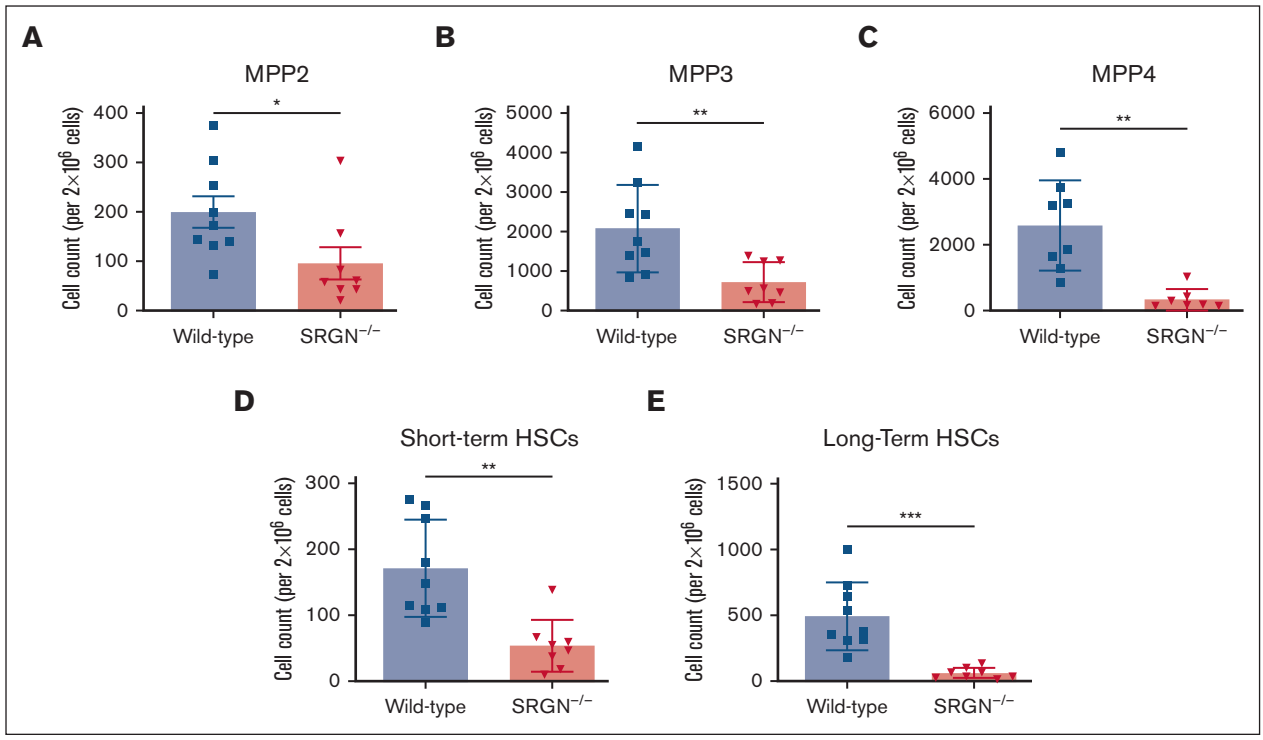

Figure 7. SRGN$^{-/-}$ mice have decreased bone marrow stem cell populations. Multipotent progenitor population cell counts determined by flow cytometry of whole marrow cells from 52-week-old mice and selection as follows: MPP2: CD45$^+$Lin$^-$Sca-1$^+$c-Kit$^+$Flt3$^-$CD150$^+$CD48$^+$ (A); MPP3: CD45$^+$Lin$^-$Sca-1$^+$c-Kit$^+$Flt3$^-$CD150$^-$CD48$^+$ (B); MPP4: CD45$^+$Lin$^-$Sca-1$^+$c-Kit$^+$Flt3$^+$ (C). Each point represents a single mouse (n = 9). (D-E) Short-term HSC (ST-HSC) (D) and long-term HSC (LT-HSC) counts (E) determined by flow cytometry of whole marrow cells from 52-week-old mice and selection as follows: LT-HSCs: CD45$^+$Lin$^-$Sca-1$^+$c-Kit$^+$Flt3$^-$CD150$^+$CD48$^-$; ST-HSCs: CD45$^+$Lin$^-$Sca-1$^+$c-Kit$^+$Flt3$^-$CD150$^-$CD48$^+$. Each point represents a single mouse (n = 9). Significance: ns is indicated by $P > .05$; *$P \leq .05$; **$P \leq .01$; ***$P \leq .001$; ****$P \leq .0001$. All error bars represent the SEM.

for cancer progression.[28,70-74] Although SRGN is traditionally classified as an intracellular proteoglycan, many studies have documented its secretion by diverse cell types, its incorporation into the extracellular matrix, and its association with the cell surface.[73-75] SRGN is uniquely positioned to regulate the availability of many key factors for stem cell and niche development because it is not anchored to a cell surface and instead could diffuse locally. Thus, SRGN is a regulatable proteoglycan that can be released by multiple cell types with specific factors already bound, allowing it to regulate a wide array of processes in the bone marrow. Our findings show that the nontoxic, small molecule surfen is useful to affect SRGN activity and thus study more of its diverse roles.

Further studies are needed to delineate the mechanism(s) by which PF4 release controls MK development. The discovery of a specific receptor or characterization of downstream signaling and expression changes could be vital to developing interventions that could target this pathway instead of the cellular-myeloproliferative leukemia protein receptor. As we continue to characterize the factors involved in sorting α-granule cargo, it is still unknown how intragranular proteins such as PF4 interact with cytosolic factors such as NBEAL2 for retention and selection. It is possible that a yet unidentified transmembrane protein binds SRGN to mediate its trafficking to the α-granule. Additionally, identification of the factors bound to SRGN in different contexts, such as different GAG modifications, tissues, inflammatory stages, cancerous vs healthy tissue, etc, would allow for identification of important binding partners and in developing interventions for manipulating growth factor or cytokine availability. However, there is a need for the development of better antibodies and technologies for working with SRGN.

Acknowledgments

The authors thank Jeremy P. Wood and the members of the Whiteheart Laboratory for their careful perusal of this manuscript and their patience. The authors are thankful for the efforts of Ming Zhang in managing the mouse colony. The authors thank the University of Kentucky Imaging Core Facility for their technical assistance with imaging experiments. The authors also thank Ann Stowe for access to her laboratory's BD Symphony A3 and Jadwiga Turchan for her technical assistance and expertise.

The work was supported by grants from the National Institutes of Health, National Heart, Lung, and Blood Institute (grants HL56652, HL138179, and HL150818), and the Department of Veterans Affairs Merit Award [S.W.W.].

Authorship

Contribution: J.L. conceived the project, performed and analyzed the experiments, and wrote the manuscript; I.C.B., V.C., H.R.A., and J.P. performed and analyzed experiments and edited the manuscript; J.I. edited the manuscript; and S.W.W. directed the research and edited the manuscript.

Conflict-of-interest disclosure: The authors declare no competing financial interests.

ORCID profiles: J.L., 0009-0002-9276-0092; I.C.B., 0000-0003-2725-8493; H.R.A., 0000-0003-4668-4367; J.I., 0000-0001-6547-9663; S.W.W., 0000-0001-5577-0473.

Correspondence: Sidney W. Whiteheart, Molecular and Cellular Biochemistry, University of Kentucky, 741 South Limestone, Lexington, KY 40536; email: whitehe@uky.edu.

References

1. Noetzli LJ, French SL, Machlus KR. New insights into the differentiation of megakaryocytes from hematopoietic progenitors. *Arterioscler Thromb Vasc Biol*. 2019;39(7):1288-1300.
2. Sharda A, Flaumenhaft R. The life cycle of platelet granules. *F1000Res*. 2018;7:236-248.
3. Malara A, Abbonante V, Zingariello M, Franco Migliaccio AR, Balduini A. Megakaryocyte contribution to bone marrow fibrosis: many arrows in the quiver. *Mediterr J Hematol Infect Dis*. 2018;10(1):e2018068.
4. Olson TS, Caselli A, Otsuru S, et al. Megakaryocytes promote murine osteoblastic HSC niche expansion and stem cell engraftment after radioablative conditioning. *Blood*. 2013;121(26):5238-5249.
5. Tilburg J, Becker IC, Italiano JE. Don't you forget about me(gakaryocytes). *Blood*. 2022;139(22):3245-3254.
6. Winter O, Moser K, Mohr E, et al. Megakaryocytes constitute a functional component of a plasma cell niche in the bone marrow. *Blood*. 2010;116(11):1867-1875.
7. Zhao M, Perry JM, Marshall H, et al. Megakaryocytes maintain homeostatic quiescence and promote post-injury regeneration of hematopoietic stem cells. *Nat Med*. 2014;20(11):1321-1326.
8. Capitano M, Zhao L, Cooper S, et al. Phosphatidylinositol transfer proteins regulate megakaryocyte TGF-β1 secretion and hematopoiesis in mice. *Blood*. 2018;132(10):1027-1038.
9. Bruns I, Lucas D, Pinho S, et al. Megakaryocytes regulate hematopoietic stem cell quiescence through CXCL4 secretion. *Nat Med*. 2014;20(11):1315-1320.
10. Abbonante V, Chitalia V, Rosti V, et al. Upregulation of lysyl oxidase and adhesion to collagen of human megakaryocytes and platelets in primary myelofibrosis. *Blood*. 2017;130(6):829-831.
11. Nakamura-Ishizu A, Takubo K, Fujioka M, Suda T. Megakaryocytes are essential for HSC quiescence through the production of thrombopoietin. *Biochem Biophys Res Commun*. 2014;454(2):353-357.
12. Pinho S, Marchand T, Yang E, Wei Q, Nerlov C, Frenette PS. Lineage-biased hematopoietic stem cells are regulated by distinct niches. *Dev Cell*. 2018;44(5):634-641.e4.
13. Ding L, Morrison SJ. Haematopoietic stem cells and early lymphoid progenitors occupy distinct bone marrow niches. *Nature*. 2013;495(7440):231-235.
14. Maynard DM, Heijnen HFG, Gahl WA, Gunay-Aygun M. The α-granule proteome: novel proteins in normal and ghost granules in gray platelet syndrome. *J Thromb Haemost*. 2010;8(8):1786-1796.
15. Maynard DM, Heijnen HFG, Horne MK, White JG, Gahl WA. Proteomic analysis of platelet α-granules using mass spectrometry. *J Thromb Haemost*. 2007;5(9):1945-1955.
16. Affandi AJ, Carvalheiro T, Ottria A, et al. CXCL4 drives fibrosis by promoting several key cellular and molecular processes. *Cell Rep*. 2022;38(1):110189.
17. Lambert MP, Meng R, Xiao L, et al. Intramedullary megakaryocytes internalize released platelet factor 4 and store it in alpha granules. *J Thromb Haemost*. 2015;13(10):1888-1899.
18. Lambert MP, Wang Y, Bdeir KH, Nguyen Y, Kowalska MA, Poncz M. Platelet factor 4 regulates megakaryopoiesis through low-density lipoprotein receptor–related protein 1 (LRP1) on megakaryocytes. *Blood*. 2009;114(11):2290-2298.
19. Lambert MP, Rauova L, Bailey M, Sola-Visner MC, Kowalska MA, Poncz M. Platelet factor 4 is a negative autocrine in vivo regulator of megakaryopoiesis: clinical and therapeutic implications. 2007;110(4):1153-1160.
20. Silva-Cardoso SC, Tao W, Angiolilli C, et al. CXCL4 links inflammation and fibrosis by reprogramming monocyte-derived dendritic cells in vitro. *Front Immunol*. 2020;11:2149-2166.
21. Gleitz HFE, Dugourd AJF, Leimkühler NB, et al. Increased CXCL4 expression in hematopoietic cells links inflammation and progression of bone marrow fibrosis in MPN. *Blood*. 2020;136(18):2051-2064.
22. Norozi F, Shahrabi S, Hajizamani S, Saki N. Regulatory role of megakaryocytes on hematopoietic stem cells quiescence by CXCL4/PF4 in bone marrow niche. *Leuk Res*. 2016;48:107-112.
23. Barber AJ, Käser-Glanzmann R, Jakábová M, Lüscher EF. Characterization of a chondroitin 4 -sulfate proteoglycan carrier for heparin neutralizing activity (platelet factor 4) released from human blood platelets. *Biochim Biophys Acta*. 1972;286(2):312-329.
24. Chanzu H, Lykins J, Wigna-Kumar S, et al. Platelet α-granule cargo packaging and release are affected by the luminal proteoglycan, serglycin. *J Thromb Haemost*. 2021;19(4):1082-1095.
25. Meen AJ, Øynebråten I, Reine TM, et al. Serglycin is a major proteoglycan in polarized human endothelial cells and is implicated in the secretion of the chemokine GROα/CXCL1. *J Biol Chem*. 2011;286(4):2636-2647.

26. Niemann CU, Cowland JB, Klausen P, Askaa J, Calafat J, Borregaard N. Localization of serglycin in human neutrophil granulocytes and their precursors. *J Leukoc Biol*. 2004;76(2):406-415.
27. Manou D, Bouris P, Kletsas D, et al. Serglycin activates pro-tumorigenic signaling and controls glioblastoma cell stemness, differentiation and invasive potential. *Matrix Biol Plus*. 2020;6-7:100033.
28. Manou D, Karamanos NK, Theocharis AD. Tumorigenic functions of serglycin: Regulatory roles in epithelial to mesenchymal transition and oncogenic signaling. *Semin Cancer Biol*. 2020;62:108-115.
29. Toyama-Sorimachi N, Kitamura F, Habuchi H, Tobita Y, Kimata K, Miyasaka M. Widespread expression of chondroitin sulfate-type serglycins with CD44 binding ability in hematopoietic cells. *J Biol Chem*. 1997;272(42):26714-26719.
30. Sutton VR, Brennan AJ, Ellis S, et al. Serglycin determines secretory granule repertoire and regulates natural killer cell and cytotoxic T lymphocyte cytotoxicity. *FEBS J*. 2016;283(5):947-961.
31. The UniProt Consortium. UniProt: the universal protein knowledgebase in 2023. *Nucleic Acids Res*. 2023;51(D1):D523-D531.
32. Lord MS, Cheng B, Farrugia BL, McCarthy S, Whitelock JM. Platelet factor 4 binds to vascular proteoglycans and controls both growth factor activities and platelet activation. *J Biol Chem*. 2017;292(10):4054-4063.
33. Kolset SO, Pejler G. Serglycin: a structural and functional chameleon with wide impact on immune cells. *J Immunol*. 2011;187(10):4927-4933.
34. Niu C, Yang Y, Huynh A, Nazy I, Kaltashov IA. Platelet factor 4 interactions with short heparin oligomers: implications for folding and assembly. *Biophys J*. 2020;119(7):1371-1379.
35. Woulfe DS, Lilliendahl JK, August S, et al. Serglycin proteoglycan deletion induces defects in platelet aggregation and thrombus formation in mice. *Blood*. 2008;111(7):3458-3467.
36. Lo RW, Li L, Leung R, Pluthero FG, Kahr WHA. NBEAL2 (Neurobeachin-like 2) is required for retention of cargo proteins by α-granules during their production by megakaryocytes. *Arterioscler Thromb Vasc Biol*. 2018;38(10):2435-2447.
37. Cao L, Su J, Li J, et al. A novel nonsense NBEAL2 gene mutation causing severe bleeding in a patient with gray platelet syndrome. *Platelets*. 2018;29(3):288-291.
38. Deppermann C, Nurden P, Nurden AT, Nieswandt B, Stegner D. The Nbeal2−/− mouse as a model for the gray platelet syndrome. *Rare Dis*. 2013;1:e26561.
39. Heib T, Gross C, Müller M-L, Stegner D, Pleines I. Isolation of murine bone marrow by centrifugation or flushing for the analysis of hematopoietic cells – a comparative study. *Platelets*. 2021;32(5):601-607.
40. Becker IC, Nagy Z, Manukjan G, et al. G6b-B regulates an essential step in megakaryocyte maturation. *Blood Adv*. 2022;6(10):3155-3161.
41. Camacho V, Guo K, Hanc P, et al. Megakaryocytes direct CD4 + T cell responses via major histocompatibility complex class II antigen presentation. *Blood*. 2023;142(suppl 1):35.
42. Okada Y, Nobori H, Shimizu M, et al. Multiple ETS family proteins regulate PF4 gene expression by binding to the same ETS binding site. *PLoS One*. 2011;6(9):e24837.
43. Pang L, Xue HH, Szalai G, et al. Maturation stage–specific regulation of megakaryopoiesis by pointed-domain Ets proteins. *Blood*. 2006;108(7):2198-2206.
44. Ambrosio AL, Febvre HP, Pietro SMD. Syntaxin 12 and COMMD3 are new factors that function with VPS33B in the biogenesis of platelet a-granules. *Blood*. 2022;139(6):922-935.
45. Ambrosio AL, Pietro SMD. Mechanism of platelet a-granule biogenesis: study of cargo transport and the VPS33B-VPS16B complex in a model system. *Blood Adv*. 2019;3(17):2617-2626.
46. Schuksz M, Fuster MM, Brown JR, et al. Surfen, a small molecule antagonist of heparan sulfate. *Proc. Natl. Acad. Sci U S A*. 2008;105(35):13075-13080.
47. Lande R, Mennella A, Palazzo R, et al. Anti-CXCL4 antibody reactivity is present in systemic sclerosis (SSc) and correlates with the SSc type I interferon signature. *Int J Mol Sci*. 2020;21(14):5102-5118.
48. Rueda F, Piñol G, Marti F, Pujol-Moix N. Abnormal levels of platelet-specific proteins and mitogenic activity in myeloproliferative disease. *Acta Haematol*. 1991;85(1):12-15.
49. Ozono Y, Shide K, Kameda T, et al. Neoplastic fibrocytes play an essential role in bone marrow fibrosis in Jak2V617F-induced primary myelofibrosis mice. *Leukemia*. 2021;35(2):454-467.
50. Meier-Abt F, Wolski WE, Tan G, et al. Reduced CXCL4/PF4 expression as a driver of increased human hematopoietic stem and progenitor cell proliferation in polycythemia vera. *Blood Cancer J*. 2021;11(2):31-37.
51. Lo RW, Li L, Pluthero FG, Leung R, Eto K, Kahr WHA. The endoplasmic reticulum protein SEC22B interacts with NBEAL2 and is required for megakaryocyte α-granule biogenesis. *Blood*. 2020;136(6):715-725.
52. Aled O'Neill, Chin D, Tan D, Abdul Majeed ABB, Nakamura-Ishizu A, Suda T. Thrombopoietin maintains cell numbers of hematopoietic stem and progenitor cells with megakaryopoietic potential. *Haematologica*. 2021;106(7):1883-1891.
53. Haas S, Hansson J, Klimmeck D, et al. Inflammation-induced emergency megakaryopoiesis driven by hematopoietic stem cell-like megakaryocyte progenitors. *Cell Stem Cell*. 2015;17(4):422-434.

54. Xavier-Ferrucio J, Krause DS. Concise review: bipotent megakaryocytic-erythroid progenitors: concepts and controversies. *Stem Cells*. 2018;36(8):1138-1145.

55. Pietras EM, Reynaud D, Kang YA, et al. Functionally distinct subsets of lineage-biased multipotent progenitors control blood production in normal and regenerative conditions. *Cell Stem Cell*. 2015;17(1):35-46.

56. Kokkaliaris KD, Kunz L, Cabezas-Wallscheid N, et al. Adult blood stem cell localization reflects the abundance of reported bone marrow niche cell types and their combinations. *Blood*. 2020;136(20):2296-2307.

57. Huang H, Cantor AB. Common features of megakaryocytes and hematopoietic stem cells: what's the connection? *J Cell Biochem*. 2009;107(5):857-864.

58. Sun S, Jin C, Si J, et al. Single-cell analysis of ploidy and the transcriptome reveals functional and spatial divergency in murine megakaryopoiesis. *Blood*. 2021;138(14):1211-1224.

59. Lu R, Neff NF, Quake SR, Weissman IL. Tracking single hematopoietic stem cells in vivo using high-throughput sequencing in conjunction with viral genetic barcoding. *Nat Biotechnol*. 2011;29(10):928-933.

60. Yamamoto R, Morita Y, Ooehara J, et al. Clonal analysis unveils self-renewing lineage-restricted progenitors generated directly from hematopoietic stem cells. *Cell*. 2013;154(5):1112-1126.

61. Hamill KJ, Kligys K, Hopkinson SB, Jones JCR. Laminin deposition in the extracellular matrix: a complex picture emerges. *J Cell Sci*. 2009;122(Pt 24):4409-4417.

62. Susek KH, Korpos E, Huppert J, et al. Bone marrow laminins influence hematopoietic stem and progenitor cell cycling and homing to the bone marrow. *Matrix Biol*. 2018;67:47-62.

63. Malara A, Currao M, Gruppi C, et al. Megakaryocytes contribute to the bone marrow-matrix environment by expressing fibronectin, type IV collagen, and laminin. *Stem Cells*. 2014;32(4):926-937.

64. Hallmann R, Horn N, Selg M, Wendler O, Pausch F, Sorokin LM. Expression and function of laminins in the embryonic and mature vasculature. *Physiol Rev*. 2005;85(3):979-1000.

65. Korpetinou A, Skandalis SS, Labropoulou VT, et al. Serglycin: at the crossroad of inflammation and malignancy. *Front Oncol*. 2014;3(3):327.

66. Kolset SO, Tveit H. Serglycin – structure and biology. *Cell Mol Life Sci*. 2008;65(7-8):1073-1085.

67. Hardingham TE, Fosang AJ. Proteoglycans: many forms and many functions. *FASEB J*. 1992;6(3):861-870.

68. Elfenbein A, Simons M. Auxiliary and autonomous proteoglycan signaling networks. *Methods Enzymol*. 2010;480:3-31.

69. Murdoch AD, Iozzo RV. Perlecan: the multidomain heparan sulphate proteoglycan of basement membrane and extracellular matrix. *Virchows Arch A Pathol Anat Histopathol*. 1993;423(4):237-242.

70. Niemann CU, Kjeldsen L, Ralfkiaer E, Jensen MK, Borregaard N. Serglycin proteoglycan in hematologic malignancies: a marker of acute myeloid leukemia. *Leukemia*. 2007;21(12):2406-2410.

71. Bouris P, Manou D, Sopaki-Valalaki A, et al. Serglycin promotes breast cancer cell aggressiveness: induction of epithelial to mesenchymal transition, proteolytic activity and IL-8 signaling. *Matrix Biol*. 2018;74:35-51.

72. Roy A, Attarha S, Weishaupt H, et al. Serglycin as a potential biomarker for glioma: association of serglycin expression, extent of mast cell recruitment and glioblastoma progression. *Oncotarget*. 2017;8(15):24815-24827.

73. Zernichow L, Abrink M, Hallgren J, Grujic M, Pejler G, Kolset SO. Serglycin is the major secreted proteoglycan in macrophages and has a role in the regulation of macrophage tumor necrosis factor-α secretion in response to lipopolysaccharide. *J Biol Chem*. 2006;281(37):26792-26801.

74. Li X-J, Qian C-N. Serglycin in human cancers. *Chin J Cancer*. 2011;30(9):585-589.

75. Melo FR, Grujic M, Spirkoski J, Calounova G, Pejler G. Serglycin proteoglycan promotes apoptotic versus necrotic cell death in mast cells. *J Biol Chem*. 2012;287(22):18142-18152.